

EXPERIMENTAL INVESTIGATION OF TWO-PHASE CLOSED THERMOSYPHON FOR LOW-TEMPERATURE GEOTHERMAL APPLICATION

Yu-jiao Lei, Jia-ling Zhu*, Yi-fan Sui, Yu-shi Wang

Key Laboratory of Efficient Utilization of Low and Medium Grade Energy of Ministry of Education (Tianjin University),
Tianjin 300350, PR China

ABSTRACT

In the conventional downhole heat transfer mode, using the two-phase closed thermosyphon (TPCT) can greatly improve the heat extraction capability from geothermal reservoirs. In this paper, a set of laboratory-scale performance testing device is built for TPCTs with internal tubes and charged with CO₂-nanofluids mixed working fluid. Based on the conditions of geothermal reservoir and heating season, experimental investigations are carried out by various heating temperature (50~70 °C), heating water flow rate (1.0~3.0m³/h), cooling temperature (5~15 °C) and cooling water flow rate (1.0~3.0m³/h). The results show that the increase of heating temperature plays a dominant part in heat transfer performance, but not always be positively correlated due to the increase in temperature difference between the evaporator section and the condenser section. From the perspective of their own structure, outer fins have the most obvious improvement on their performance and another method of reducing the aspect ratio takes second place.

Keywords: geothermal energy, two-phase closed thermosyphon (TPCT), CO₂-nanofluids, heat transfer performance

NONMENCLATURE

Abbreviations

TPCT Two-phase closed thermosyphon

Symbols

D External diameter(mm)
d Internal diameter(mm)
L Length(mm)
T Temperature(°C)

ΔT	Temperature difference(°C)
V	Water flow rate(m ³ /h)
Q	Heat transfer rate(kW)
ρ	Water density(kg/m ³)
c_p	Specific heat capacity[kJ/(kg.K)]
λ	Thermal conductivity[W/(m.K)]
R	Thermal resistance(K/W)
h_{eff}	Equivalent convective heat transfer coefficient[kW/(m ² .K)]

Subscripts

eva	Evaporator
con	Condenser
h	Heating
c	Cooling
in	Inlet
out	Outlet

1. INTRODUCTION

Geothermal energy is a type of clean, stable and renewable energy. In the southeast coast and internal basin areas of China, low temperature geothermal resources (≤ 90 °C) are largely reserved, widely distributed and have been used for space heating in recent years [1]. Compared with the traditional geothermal application methods with geo-fluid extraction, the two-phase closed thermosyphon (TPCT) doesn't need the return irrigation of geothermal water and can avoid the corrosion and scaling of pipes [1][2]. The TPCT's working mechanism is the phase transition and circulation of the working fluid inside. Different from wicked heat pipes, the condensate returning to the evaporator section is assisted by gravity in TPCTs. Therefore, the TPCT also has advantages of higher effectiveness, simpler structure, no external drive and better isothermal characteristics by phase change heat

transfer than circulation pipes (e.g. coaxial pipes, U-shaped pipes).

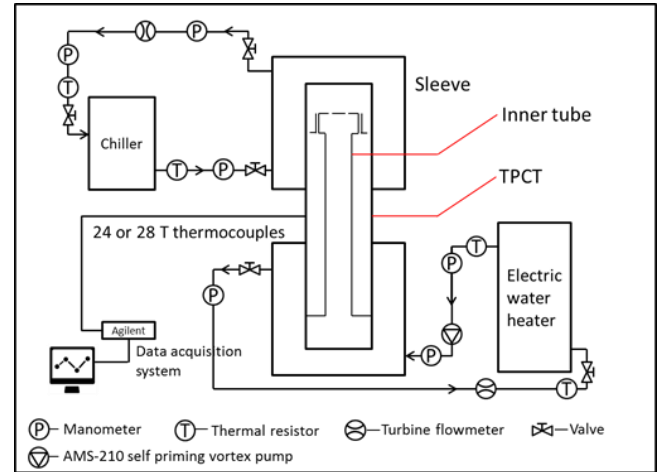
Recent researches on TPCTs are mainly used for waste heat recovery [3], ground temperature control [4], heat dissipation of electronic apparatus [5][6], and solar energy[7][8], etc. In the existing papers, the reliability of nanofluids [9-11] and liquid CO₂ [12][13] as the working fluid of thermosyphon has been proved effective, respectively. In my experimental investigation, the three TPCTs are filled with 30% nanofluids and 70% liquid CO₂ as working fluid, ensuring the boiling heat transfer under the temperature below 90°C. At the same time, each TPCT is internally fitted with a coaxial tube to avoid the occurrence of entrainment limit.

2. EXPERIMENTS

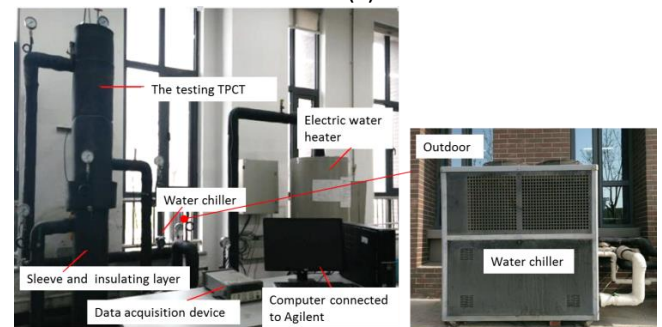
2.1 Experimental setup and procedure

As shown in Fig.1 (a) and (b), the entire experimental process of the system is carried out in the vertical direction. The experimental system consists of the TPCT, electric water heater, air-to-water chiller, two water loops and data acquisition system, etc. The relevant parameters are summarized in Table.1. Among them, the #F1 is equipped with outer spiral fins while #B1 and #B2 are bare tubes.

In the experimental system, an electric water heater (Type DRE-80-54) is used as a basically constant heating source and an air-to-water chiller (Type AC-08AD) simulates the user side to provide cooling water. In each of the circulating lines, a liquid turbine flowmeter is installed to measure the volume flow rate and four PT100 thermal resistors are inserted into the tubes to measure the water temperature of the inlet and outlet. In order to obtain the condensation temperature and evaporation temperature of the TPCT, 12 or 14 pairs of T-type thermocouples are welded onto its outer wall to measure the real-time temperature. The wall temperature fluctuation bellow 0.5°C marks the steady operation of experimental system.



(a)



(b)

Fig 1 (a) The schematic diagram (b) The physical connection diagram of the experimental system

Table 1 Main parameters of the TPCTs

Property	#B1	#F1	#B2
Material	Carbon steel		
D (mm)	110		
d (mm)	98		
L (mm)	2000	2000	1600
L _{eva} (mm)	950	950	750
L _{con} (mm)	950	950	750
T _{h,in} (°C)	50-60-70		
V _h (m ³ /h)	1.0-1.5-2.0-2.5-3.0		
T _{c,in} (°C)	5-10-15		
V _c (m ³ /h)	1.0-2.0-3.0		

2.2 Data processing

According to the measured pipe flow and inlet and outlet temperature, the heat flux at the evaporator and the condenser can be calculated as:

$$Q_h = \rho V_h c_{p,h} (T_{h,in} - T_{h,out}) \quad (1)$$

$$Q_c = \rho V_c c_{p,c} (T_{c,out} - T_{c,in}) \quad (2)$$

The average heat transfer rate of the system is determined as:

$$Q = (Q_h + Q_c)/2 \quad (3)$$

The equivalent convective heat transfer coefficient is used as an evaluation the TPCTs' thermal performance. It is the weighted average of the boiling heat transfer coefficient and the condensation heat transfer coefficient, and reflects the two heat transfer processes comprehensively. It can be calculated using the following equations:

$$h_{eff} = \frac{2\lambda Q(L_{eva} + L_{con})}{2\pi\lambda d\Delta T L_{eva}L_{con} - Qd(L_{eva} + L_{con})\ln(D/d)} \quad (4)$$

$$\Delta T = T_{eva} - T_{con} \quad (5)$$

T_{eva} and T_{con} are the average wall temperatures measured by wall-welded thermocouples of the evaporator section and condenser section, respectively.

$$\frac{\Delta Q}{Q} = \sqrt{\left(\frac{\delta V}{V}\right)^2 + \frac{\delta^2(T_{in}) + \delta^2(T_{out})}{(T_{in} - T_{out})^2}} \quad (6)$$

$$\frac{\Delta(h_{eff})}{h_{eff}} = \sqrt{\left(\frac{\delta Q}{Q}\right)^2 + \frac{\delta^2(\bar{T}_{eva}) + \delta^2(\bar{T}_{con})}{(\bar{T}_{eva} - \bar{T}_{con})^2}} \quad (7)$$

According to equation 6 and 7, the maximum uncertainties for the heat transfer rate and the equivalent heat transfer coefficient are calculated within 7.15% and 11.37%.

3. RESULTS AND DISCUSSION

3.1 The effect of operation conditions

When the TPCTs are in stable operation, the heat exchange efficiency (Equation.6) ranges from 85% to 105%, which is caused by heat loss and measurement error. Owing to this ignorable difference, the average heat transfer rate is taken to measure the heat transfer capacity of the TPCT comprehensively.

$$\eta = \frac{Q_c}{Q_h} \times 100\% \quad (8)$$

Fig.2 and Fig.3 show the average heat transfer rate and the equivalent convective heat transfer coefficient in #B1 TPCT with various heating conditions. With the increase of heating water flow rate, the heat transfer rate and the equivalent convective heat transfer coefficient present an upward linear trend overall. However, under a larger heating temperature, the heat transfer rate is improved largely while the equivalent

convective heat transfer coefficient goes down. It can be explained that as the heat input increases, the forced convection heat transfer is enhanced, but due to the low-boiling-temperature working fluid, the boiling heat transfer has been fully developed under the temperature of 50 °C . The increase of heating temperature can not only increase the heat transfer rate, but also increases ΔT to a greater extent.

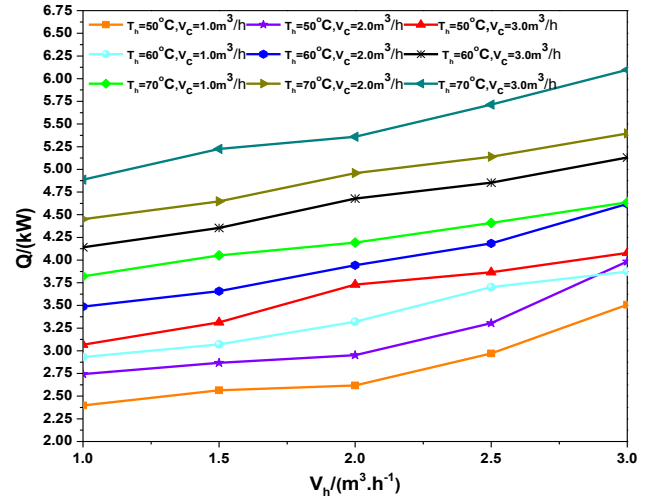


Fig 2 The change trend of average heat transfer rate under various heating conditions in #B1 TPCT.($T_c=10^\circ\text{C}$)

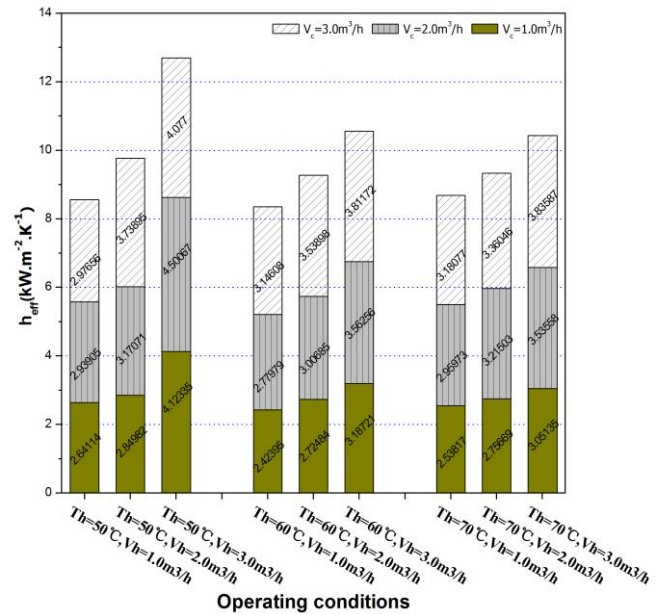


Fig 3 The equivalent convective heat transfer coefficient under various heating conditions in #B1 TPCT.($T_c=10^\circ\text{C}$)

Fig.4 and Fig.5 show the change of average heat transfer rate and the equivalent convective heat transfer coefficient in #B1 TPCT with various cooling conditions. It can be obtained that the decrease in cooling temperature and increase in cold water flow

rate are positively correlated with the heat transfer performance of the TPCT. Both of these parameter changes represent an enhancement in cooling capacity. As a direct consequence, the circulation of the working fluid in the TPCT is accelerated and the heat transfer rate increases. In addition, the quality of condensate reflux increases, the inner wall surface can be more uniformly covered, which results in the increase of effective heat exchange area. Comparing the two methods of increasing the flow rate and lowering the cooling temperature, it can be seen that the former has a greater improvement on the equivalent convective heat transfer coefficient. Similar to the discussion of heat sources above, directly changing the temperature can increase ΔT to a large extent.

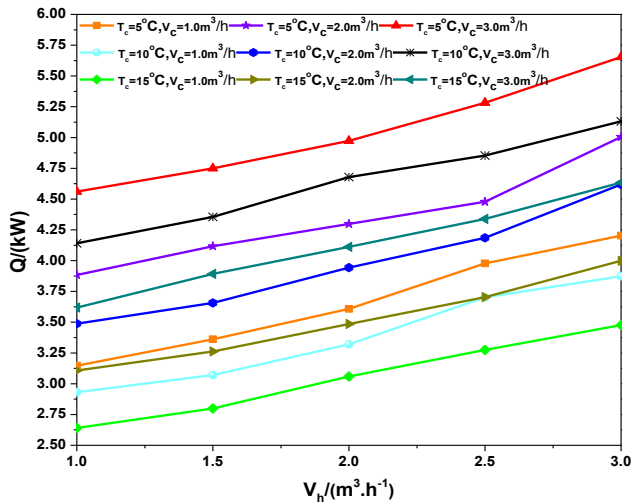


Fig 4 The change trend of average heat transfer rate under various cooling conditions in #B1 TPCT. ($T_h=60^\circ\text{C}$)

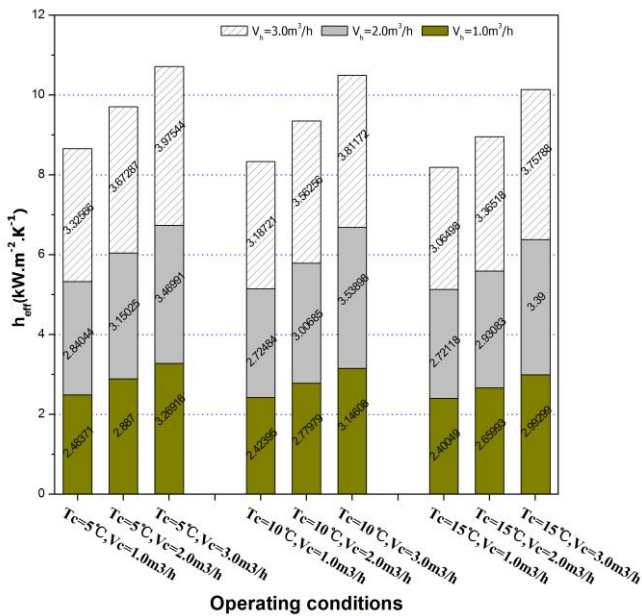


Fig 5 The equivalent convective heat transfer coefficient under various cooling conditions in #B1 TPCT. ($T_h=60^\circ\text{C}$)

3.2 The effect of structure of TPCTs

As Fig.6 shows, the axial temperature distribution of external finned TPCT (#F1) does not constantly decrease or rise, but in fluctuation. In comparison, the wall temperature of the bare TPCT (#B1) drops along the evaporator and rises along the condenser more continuously. This is mainly due to the resistance and disturbance of the outer fins to water. At the same time, combining the Fig.8, it can be concluded that the increase of the effective heat exchange area and the disturbance to the water flow by outer fins greatly improve the heat transfer performance of the TPCT. From another point of view, it can also be considered that the internal boiling heat transfer coefficient is much larger than the external convective heat transfer coefficient, so enhancing the heat transfer outside the TPCT is of great significance for the improvement of overall heat transfer capacity. It should be noted that the large temperature difference between the 7th and 8th measuring points is due to the fact that the heating and the cooling water both enter in the bottom and leave at top in the sleeve, but not the heat transfer performance of the TPCTs.

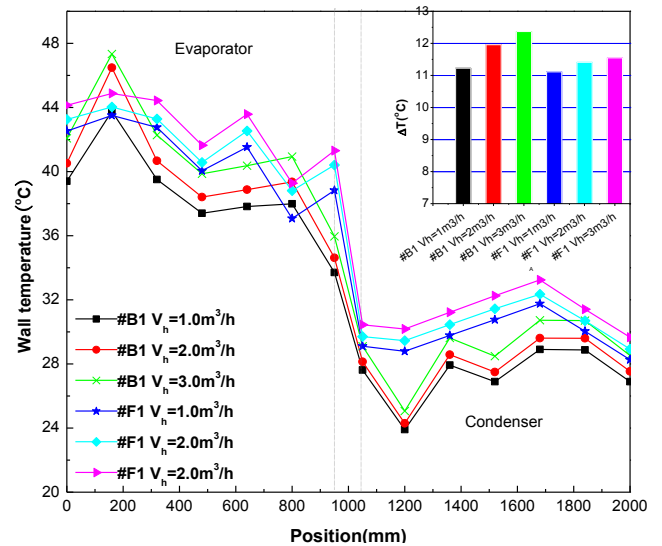


Fig 6 Wall temperature distribution and the temperature difference between evaporator and condenser of the #B1 and #F1 TPCTs ($T_h=60^\circ\text{C}, T_c=10^\circ\text{C}, V_c=2.0\text{m}^3/\text{h}$)

In Fig.7, #B1 ($L=2000\text{mm}$) and #B2 ($L=1600\text{mm}$) TPCTs have similar wall temperature change trend, but the former has a larger temperature difference between evaporator and condenser. As a consequence, even #B1 TPCT has 1.45~1.67 times the heat transfer rate of #B2 TPCT; its equivalent convective heat transfer coefficient is lower than that of #B2 TPCT (Fig.8). On the whole, the main reason of the higher heat transfer rate

is the advantage of #B1 TPCT's larger heat exchange area. However, from the perspective of the internal heat transfer mechanism, under the same heat source conditions, the driving force for the vaporization of the working fluid is limited. So the vapor has been condensed and begins to return before reaching the top of #B1 TPCT. In Fig.7, the temperature drop at the position 1840mm to 2000mm also confirms this view, which results in reduction of heat flux density and average temperature of the condenser section.

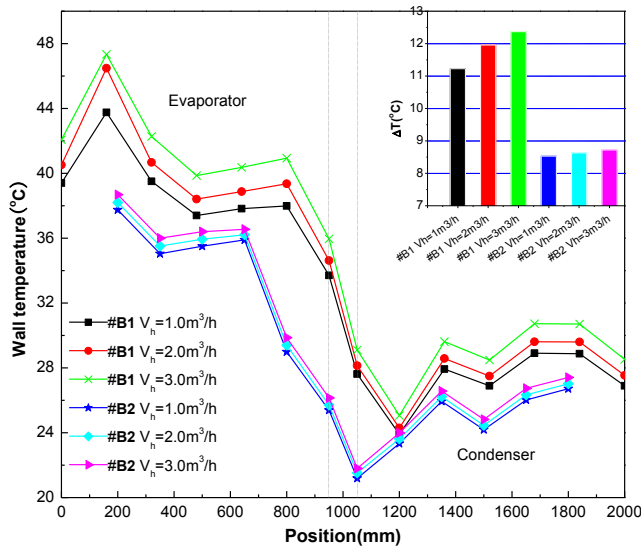


Fig 7 Wall temperature distribution and the temperature difference between evaporator and condenser of the #B1 and #B2 TPCTs ($T_h=60^\circ\text{C}, T_c=10^\circ\text{C}, V_c=2.0\text{m}^3/\text{h}$)

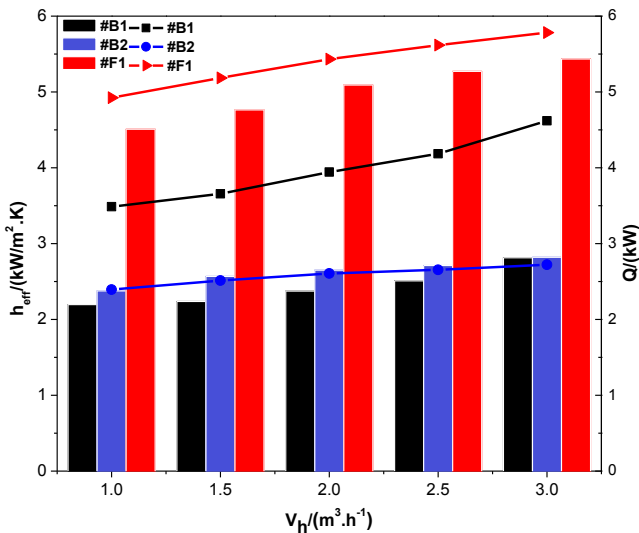


Fig 8 The average heat transfer rate (lines with symbols) and the equivalent convective heat transfer coefficient (columns) of #B1, #B2 and #F1 TPCTs under different heating flow rate ($T_h=60^\circ\text{C}, T_c=10^\circ\text{C}, V_c=2.0\text{m}^3/\text{h}$)

3.3 Conclusions

In this work, a new type of TPCT filled with CO_2 and nanofluids for geothermal application is proposed. Three TPCTs with different structure are experimentally tested under various heating temperature, cooling temperature and the water flow rate of two circulating lines. Associated with the practical application in geothermal engineering, the following points are summarized eventually.

1) The heating temperature and water flow rate play a major role in the heat transfer performance of the TPCT. The larger the heat flux in the evaporation section, the higher the average heat transfer rate, but according to the equivalent convective heat transfer coefficient, the heat transfer performance per unit area and isothermal characteristics are negatively correlated with the heating temperature. Therefore, in the design stage of TPCTs, the internal pressure should be adjusted according to the temperature condition of the geothermal reservoir, so that the boiling point of the working fluid is consistent with it.

2) Decreasing the cooling temperature and increasing cooling water flow rate are beneficial to the heat transfer performance of TPCTs. The former is related to the ambient temperature of the local heating season, while the latter is related to the quantity of users. The number of users should be increased while ensuring sufficient temperature rise.

3) The finned TPCT has obvious advantages in heat transfer performance and is suitable for geothermal systems of convective type, but there are difficulties in engineering installation. This also shows that reducing the thermal resistance between the outer wall and heat source can be an improvement direction for the geothermal application of TPCTs.

4) Under certain heat source conditions, limited by the carrying limit, the heat transfer capacity of 2000mm-long #B1 TPCT is weaker than the 1600mm-long one. Sometimes the depth of the low temperature geothermal reservoirs can be more than 400m, so the use of the ultra-long TPCT necessarily requires a stronger driving force. Magnetic nanofluids and magnetic fields will be taken as the direction of our further study.

ACKNOWLEDGEMENT

The authors gratefully acknowledge the financial support provided by the National High Technology Research and Development Program of China (863 Program) (Grant No. 2012AA053001).

REFERENCE

- [1] Tian TS, Li ML, Bai Y. China's geothermal resources and the exploitation. 1th ed. Beijing: China Environmental Science Press; 2006.
- [2] DiPippo R. Geothermal Power Plants, 2nd ed. Elsevier, Oxford; 2008. DOI:10.1016/B978-0-7506-8620-4.X5001-1.
- [3] Gedika E, Yilmaz M, Kurt H. Experimental investigation on the thermal performance of heat recovery system with gravity assisted heat pipe charged with R134a and R410A. Appl. Therm. Eng 2016; 99 :334-342. DOI:10.1016/j.applthermaleng.2015.12.075.
- [4] Kalogirou SA, Agathokleous R, Barone G, et al. Development and validation of a new TRNSYS Type for thermosiphon flat-plate solar thermal collectors: energy and economic optimization for hot water production in different climates. Renew Energy 2019; 136: 632-644. DOI:10.1016/j.renene.2018.12.086.
- [5] Yue C, Zhang Q, Zhai ZQ, et al. Numerical investigation on thermal characteristics and flow distribution of a parallel micro-channel separate heat pipe in data center. Int J Refrige-Revue Int Du Froid 2019;98:150-160. DOI:10.1016/j.ijrefrig.2018.10.025.
- [6] Chauhan A, Kandlikar SG. Characterization of a dual taper thermosiphon loop for CPU cooling in data centers. Appl Therm Eng 2019; 146:450-458. DOI:10.1016/j.applthermaleng.2018.10.010.
- [7] Pei WS, Zhang MY, Li SY, et al. Laboratory investigation of the efficiency optimization of an inclined two-phase closed thermosyphon in ambient cool energy utilization. Renew Energy 2019;133:1178-1187. DOI:10.1016/j.renene.2018.08.078.
- [8] Wenceslas KY, Ghislain T. Experimental Validation of Exergy Optimization of a Flat-Plate Solar Collector in a Thermosyphon Solar Water Heater. Arabian J Sci Eng 2019;44(3):2535-2549. DOI:10.1007/s13369-018-3227-x.
- [9] Liu ZH, Yang XF, Guo GL. Effect of nanoparticles in nanofluid on thermal performance in a miniature thermosyphon. J Appl Phys 2007;102:013526-1-8. DOI: 10.1063/1.2748348.
- [10] Shanbedi M, Heris SZ, Baniadam M, et al. Investigation of heat-transfer characterization of EDA-MWCNT/DI-water nanofluid in a two-phase closed thermosyphon. Ind Eng Chem Res 2012;51(3):1423-1428. DOI:10.1021/ie202110g.
- [11] Sarafraz MM, Pourmehran O, Yang B, et al. Assessment of the thermal performance of a thermosyphon heat pipe using zirconia-acetone nanofluids. Renew Energy 2019;136:884-895. DOI:10.1016/j.renene.2019.01.035.
- [12] Ochsner K. Carbon dioxide heat pipe in conjunction with a ground source heat pump (GSHP). Appl Therm Eng 2008;28:2077-2082. DOI:10.1016/j.applthermaleng. 2008.04.023.
- [13] Ebeling JC, Kabelac S, Luckmann S, et al. Simulation and experimental validation of a 400 m vertical CO₂ heat pipe for geothermal application. Heat Mass Transfer 2017; 53 (11):3257-3265. DOI:10.1007/s00231-017-2014-7.